

Supporting information 1 for: Cortical ignition dynamics is tightly linked to the core organization of the human connectome

Samy Castro^{1,2,*}, Wael El-Deredy³, Demian Battaglia^{4,#} and Patricio Orio^{1,#}

¹ *Centro Interdisciplinario de Neurociencias de Valparaíso, Universidad de Valparaíso, Valparaíso, Chile*

² *Programa de Doctorado en Ciencias, mención Neurociencia, Universidad de Valparaíso, Valparaíso, Chile.*

³ *Centro de Investigación y Desarrollo en Ingeniería en Salud, Universidad de Valparaíso, Valparaíso, Chile*

⁴ *Aix-Marseille Université, Institut de Neurosciences des Systèmes, INSERM UMR 1106, Marseille, France*

*First authorship; # Shared last authorship

E-mail: patricio.orio@uv.cl (PO); demian.battaglia@univ-amu.fr (DB)

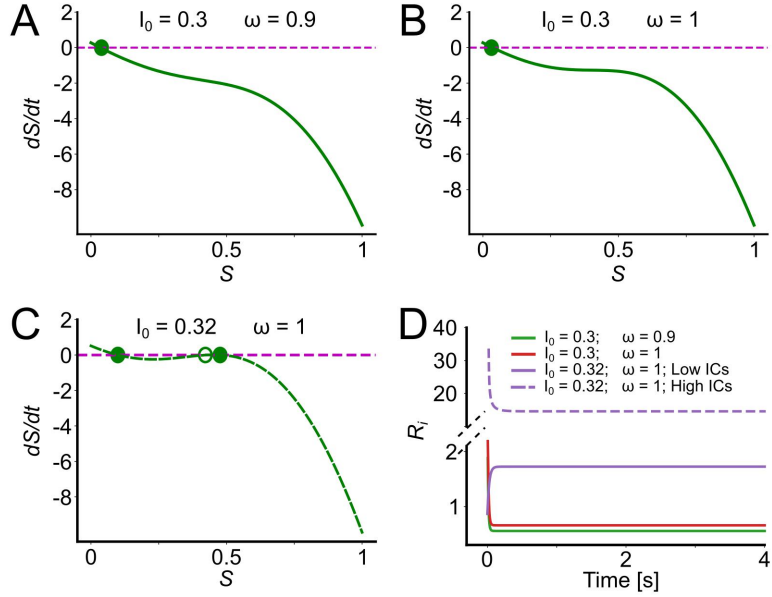


Fig A. Phase portrait and time-series of an isolated cortical area using the mean-field model.

(A-C) Three solutions as a function of I_0 and ω for an isolated node (**A** ($I_0=0.3$; $\omega=0.9$), **B** ($I_0=0.3$; $\omega=1$), and **C** ($I_0=0.32$; $\omega=1$)). The dynamics of the isolated node gets two attractors in **C**. **(D)** Mean firing rate (*y-axis*) in time (*x-axis*) for the three sets of parameters. In *purple* (the isolated region with two attractors), segmented and solid lines are simulations started from High ICs ($0.9 \leq S_i \leq 1$) or Low ICs ($0 \leq S_i \leq 0.01$), respectively. The mean-field model (MFM) with a single attractor (*green* and *red*) only displays a low mean firing rate.

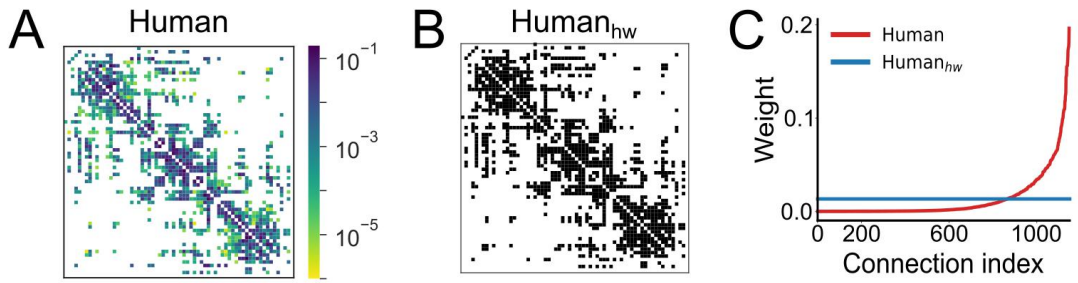


Fig B. The *Human_{hw}* connectome.

(A-B) The structural connectivity matrix of **(A)** *Human* and **(B)** *Human_{hw}* (with homogeneous weights in its connections). **(C)** Sorted connection weights of *Human* (red) and *Human_{hw}* (blue) connectomes. Note the structural heterogeneity in the *Human*. Both connectomes have 1148 connections, and 15.3 of overall strength.

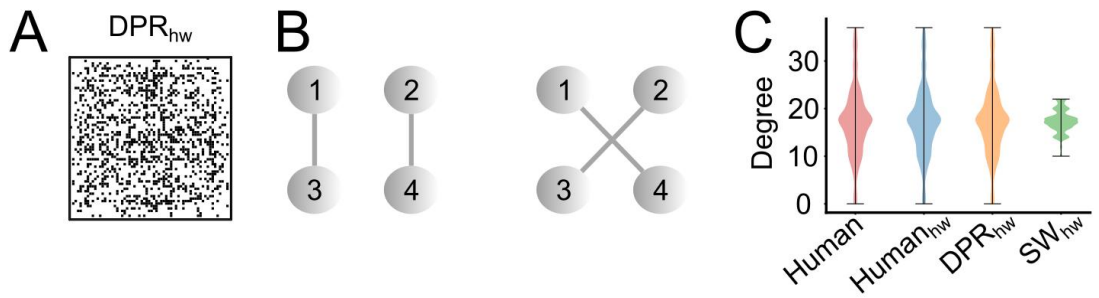


Fig C. The DPR_{hw} connectome.

(A) One representative example of the Degree-Preserving Random (DPR_{hw}) structural connectivity matrix with homogeneous weights. **(B)** An illustrative example of the Maslov & Sneppen algorithm, adapted from Fornito et al., 2016. The algorithm was applied one hundred times to the *Human* to build the DPR_{hw} connectomes. **(C)** Degree distribution of *Human*, $Human_{hw}$, DPR_{hw} , and SW_{hw} . DPR_{hw} connectomes have the same degree distribution, the number of connections (1148), and overall strength (15.3) of the *Human*.

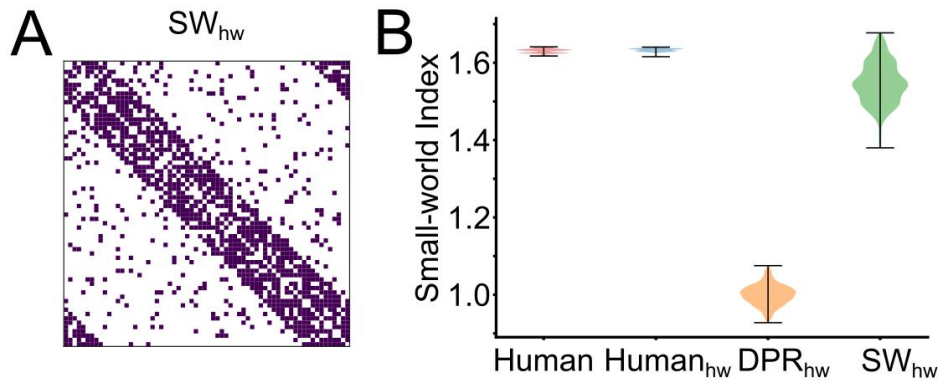


Fig D. The SW_{hw} connectome.

(A) One representative example of the Small-World (SW_{hw}) structural connectivity matrix with homogeneous weights. **(B)** Small-world index of *Human*, $Human_{hw}$, DPR_{hw} , and SW_{hw} . Note that the precise value of the small-world index depends on the random network used to normalize. Thus, its value is not deterministic, as shown by the error bars of the *Human*. The SW_{hw} connectomes conserve the number of connections (1148), and overall strength (15.3) of the *Human*.

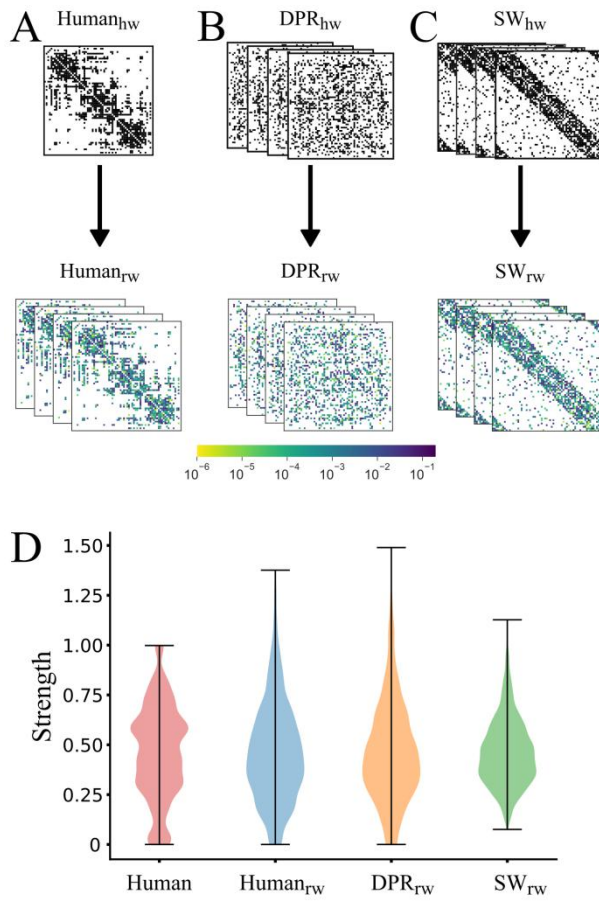


Fig E. The weighted surrogate models conserve the weight distribution of the *Human*.

The values were assigned by random permutation of *Human* connections to create: **(A)** 60 Human_{rw} from Human_{hw} ; **(B)** 60 DPR_{rw} , from 60 DPR_{hw} ; and **(C)** 60 SW_{rw} , from 60 SW_{hw} . **(D)** Strength distribution of *Human*, Human_{rw} , DPR_{rw} , and SW_{rw} .

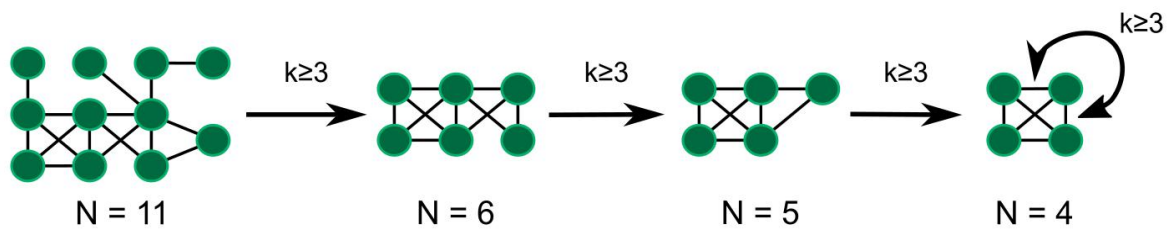


Fig F. Diagram of the k -core *decomposition* algorithm.

The k -core decomposition is used to extract the unweighted core nodes in the networks. In each step, the nodes (N) that have a degree $< k_i$ are removed in successive steps until the sub-set remains constant. The four core nodes are interconnected with $k_i \geq 3$ and thus this constitutes the 3-core. In the case of weighted networks, the s -core decomposition extracts the core nodes based on their strength ($\leq s_i$).

Table A. Abbreviations and names of cortical areas from Desikan-Killiany atlas. Adapted from Hansen et al., 2015.

Abbreviation	Cortical Area
ENT	Entorinal cortex
PARH	Parahippocampal cortex
TP	Temporal pole
FP	Frontal pole
FUS	Fusiform gyrus
TT	Transverse temporal cortex
LOCC	Lateral occipital cortex
SP	Superior parietal cortex
IT	Inferior temporal cortex
IP	Inferior temporal cortex
SMAR	Supramarginal gyrus
BSTS	Bank of the superior temporal sulcus
MT	Middle temporal cortex
ST	Superior temporal cortex
PSTC	Postcentral gyrus
PREC	Precentral gyrus
CMF	Caudal middle frontal cortex
POPE	Pars opercularis
PTRI	Pars triangularis
RMF	Rostral middle frontal cortex
PORB	Pars orbitalis
LOF	Lateral orbitofrontal cortex
CAC	Caudal anterior cingulate cortex
RAC	Rostral anterior cingulate cortex
SF	Superior frontal cortex
MOF	Medial orbitofrontal cortex
LING	Lingual gyrus
PCAL	Pericalcarine cortex
CUN	Cuneus
PARC	Paracentral lobule
ISTC	Isthmus of the cingulate cortex
PCUN	Precuneus
PC	Posterior cingulate cortex

Table B. The identity of the ignited cortical areas at the bifurcation point G..

Hagmann dataset, based on DKA parcellation has 11 cortical areas ignited (Hagmann et al., 2008). Schriner dataset, based on DKA parcellation has 12 cortical areas ignited (Schriner et al., 2015). Deco dataset (Deco et al., 2018), based on AAL parcellation (Rolls et al., 2015) has 9 cortical areas ignited. Left (**L**) and Right (**R**) hemisphere.

Hagmann dataset	Schriner dataset	Deco dataset
Pericalcarine Cortex (PCAL) L / R	Pericalcarine Cortex (PCAL) R	-
Cuneus (CUN) L / R	-	-
Paracentral Lobule (PARC) L	Paracentral Lobule (PARC) R	-
Isthmus of the Cingulate Cortex (ISTC) L / R	Isthmus of the Cingulate Cortex (ISTC) L	-
Precuneus (PCUN) L / R	-	Precuneus (PCUN) R
Posterior Cingulate Cortex (PC) L / R	-	-
-	Temporal pole (TP) R	-
-	Lateral Occipital Cortex (LOCC) R	-
-	Pars Orbitalis (PORB) R	-
-	Caudal Anterior Cingulate Cortex (CAC) R	-
-	Lingual Gyrus (LING)	-

	L	
-	Supramarginal Gyrus (SMAR) L	Supramarginal Gyrus (SMG) R
-	Middle Temporal Cortex (MT) L	-
-	Transverse Temporal Cortex (TT) L	-
-	Frontal Pole (FP) L	-
-	-	Posterior Cingulate Gyrus (PCC) L
-	-	Parahippocampal Gyrus (PHG) L
-	-	Hippocampus (HIP) L
-	-	Calcarine Fissure (CAL) L
-	-	Inferior Parietal Gyrus (IPG) L
-	-	Inferior Temporal Gyrus (ITG) R
-	-	Angular Gyrus (ANG) R